CrossMark

ORIGINAL ARTICLE

Expression of VISTA correlated with immunosuppression and synergized with CD8 to predict survival in human oral squamous cell carcinoma

Lei Wu[1] · Wei-Wei Deng[1] · Cong-Fa Huang[1] · Lin-Lin Bu[1] · Guang-Tao Yu[1] ·
Liang Mao[1] · Wen-Feng Zhang[1,2] · Bing Liu[1,2] · Zhi-Jun Sun[1,2]

Abstract V-domain Ig suppressor of T cell activation (VISTA), a novel immune checkpoint regulatory molecule, suppresses T cell mediated immune responses. The aim of the present study was to profile the immunological expression, clinical significance and correlation of VISTA in human oral squamous cell carcinoma (OSCC). Human tissue microarrays, containing 165 primary OSCCs, 48 oral epithelial dysplasias and 43 normal oral mucosae, were applied to investigate the expression levels of VISTA, CD8, cytotoxic T lymphocyte-associated antigen 4 (CTLA-4), programmed death ligand 1 (PD-L1), PI3Kα p110, IL13Rα2, phospho-STAT3 at tyrosine 705 (p-STAT3) and myeloid-derived suppressor cell (MDSC) markers (CD11b and CD33) by immunohistochemistry and digital pathology analysis. The results demonstrated that the protein level of VISTA was significantly higher in human OSCC specimens, and that VISTA expression in primary OSCCs was correlated with lymph node status. VISTA expression did not serve as an independent predictor for poor prognosis, while patient subgroup with VISTA high and CD8 low expression (22/165) had significantly poorer

overall survival compared with other subgroups based on the multivariate and Cox hazard analyses among the primary OSCC patients in the present cohort. Additionally, the expression of VISTA was significantly correlated with PD-L1, CTLA-4, IL13Rα2, PI3K, p-STAT3, CD11b and CD33 according to Pearson's correlation coefficient test. Taken together, the results indicated that the VISTA high and CD8 low group, as an immunosuppressive subgroup, might be associated with a poor prognosis in primary OSCC. These findings indicated that VISTA might be a potential immunotherapeutic target in OSCC treatment.

Keywords Immune checkpoint · VISTA · CD8 · Prognosis · Oral squamous cell carcinoma

Abbreviations

CTLA-4	Cytotoxic T lymphocyte-associated antigen 4
HPV	Human papillomavirus
MDSCs	Myeloid-derived suppressor cells
OSCC	Oral squamous cell carcinoma
PD-1	Programmed death-1
PD-L1	Programmed death ligand 1
TAMs	Tumor-associated macrophages
TPF	Cisplatin, docetaxel and fluorouracil
Tregs	Regulatory T cells
VH CH	VISTA high CD8 high
VH CL	VISTA high CD8 low
VISTA	V-domain Ig suppressor of T cell activation
VL CH	VISTA low CD8 high
VL CL	VISTA low CD8 low

L. Wu and W.-W. Deng have contributed equally to this work.

✉ Zhi-Jun Sun
zhijundejia@163.com

1 The State Key Laboratory Breeding Base of Basic Science of Stomatology and Key Laboratory of Oral Biomedicine, Ministry of Education, Wuhan University, Wuhan, China

2 Department of Oral Maxillofacial-Head Neck Oncology, School and Hospital of Stomatology, Wuhan University, Wuhan, China

Introduction

Oral squamous cell carcinoma (OSCC) is one of the ten most prevalent cancers worldwide [1]. Unfortunately, the 5-year survival rate of patients with OSCC has not been markedly improved in recent decades, but the quality of life for OSCC patients has increased as a result of more advanced therapeutic techniques [2–4]. Recently, immunotherapy has been demonstrated as a new and attractive approach, reflecting the emergence of immune checkpoint blockade with monoclonal antibodies as a successful treatment for cancer patients, including head and neck squamous carcinoma [5]. However, the molecular mechanisms of immunoregulation for OSCC are not fully understood, and the immunological molecular classification of OSCC remains uncertain.

The strategy of cancer treatment is changing, reflecting significant progress in cancer immunotherapy in recent years [6, 7]. Immune checkpoint blockade is achieved using a "common denominator" approach [8]. Immune responses against foreign pathogens or self-antigens are regulated by a balance of positive and negative molecules and pathways, such as the B7 family [9]. B7-1 and B7-2 provide critical co-stimulatory signals for T cell activation, while cytotoxic T lymphocyte-associated antigen 4 (CTLA-4), programmed death 1 (PD-1) and ligand 1 (PD-L1) down-regulate T cell responses [9, 10]. Importantly, a multitude of clinical trials have shown immune checkpoint blockade with monoclonal antibodies as markedly successful for patients with advanced melanoma, renal cell carcinoma, and relapsed follicular lymphoma [11–13]. These events fueled an intense examination of immune checkpoint molecules and suggested that immune checkpoint blockade is worthy of further studies in diverse cancer types, including OSCC.

V-domain Ig suppressor of T cell activation (VISTA), a newly identified Ig domain-containing immune checkpoint molecule, suppresses T cell mediated immune responses in vitro and in vivo [14, 15]. Previous studies have shown that VISTA blockade enhanced the activation of T cells by a VISTA monoclonal antibody in the B16 melanoma model [16]. VISTA is expressed on hematopoietic cells and myeloid cells, including neutrophils, monocytes, macrophages and dendritic cells [8]. VISTA expressed on antigen presenting cells or the soluble VISTA-Ig fusion protein inhibits the proliferation of T cells and production of cytokines [14]. VISTA gene deletion led to the gradual accumulation of spontaneously activated T cells in mice, accompanied by the production of a spectrum of inflammatory cytokines and chemokines [17]. However, the expression of VISTA has not yet been examined in OSCC.

In the present study, we examined the expression of VISTA in human OSCC tissue microarrays using digital pathology analysis and analyzed its association with pathological features and clinical significance. In addition, the correlation of VISTA expression with PD-L1, CTLA-4, PI3Kα p110, IL13Rα2, Phospho-STAT3 at Tyrosine 705 (p-STAT3) and myeloid-derived suppressor cell (MDSC) markers (CD11b and CD33) was also evaluated.

Materials and methods

Ethics statement

This study was approved by the Medical Ethics Committee of Hospital of Stomatology Wuhan University (PI: Zhi-Jun Sun) and was performed according to the Institutional Guidelines. Written informed consent was obtained from all patients.

Human OSCC tissue microarrays

The human OSCC specimen tissue microarrays used in the present study were obtained from 2008 to 2010 and 2012 to 2015 at the Department of Oral and Maxillofacial Surgery, School and Hospital of Stomatology Wuhan University. All patients histologically diagnosed as OSCC by two independent pathologists were included in the present study. The samples included all patients treated during these periods. The clinical follow-up was continuously ongoing until death. Hospital records, pathology reports, and histology slides of all patients were retrieved and reviewed. The clinical stages of the OSCC were classified according to the guidelines of the International Union against Cancer (UICC 2002). The grading scheme of the World Health Organization was used to determine the histologic grading. The clinicopathological characteristics of the cohort are shown in Supplementary Table 1. The OSCC cancer cohort consisted of 43 normal oral mucosae, 48 oral epithelial dysplasias, 165 primary OSCC patients (excluding recurrent, pre-surgical inductive chemotherapy or pre-surgical radiotherapy), 12 recurrent OSCC patients, 10 OSCC patients who received pre-surgical radiotherapy (without pre-surgical chemotherapy), 17 OSCC patients who received pre-surgical TPF (cisplatin, docetaxel and fluorouracil) inductive chemotherapy without pre-surgical radiotherapy by Zhang's protocol [18], and 41 metastatic lymph nodes. Clinical features, including TNM stage, histological grade and overall survival, were available for all cases.

Immunohistochemistry, digital pathology and scoring system

The methods and processes of immunohistochemistry were previously reported [19, 20]. Briefly, all OSCC tissue microarrays were cut into 4-μm sections. The slides were

deparaffinized and rehydrated. The sections were boiled in 0.01 M citric acid buffer solution (pH 6.0) or 1 mM EDTA buffer solution (pH 8.0) for 1.5 min at high pressure. Subsequently, the samples were incubated with 3% hydrogen superoxide for 20 min to quench endogenous peroxidase activity, and 10% goat serum was used to block non-specific binding. The sections were incubated with anti-human VISTA (Cell Signaling Technology, 1:400), PD-L1 (Cell Signaling Technology, 1:100), CTLA-4 (Santa Cruz Biotechnology, 1:200), PI3Kα p110 (Cell Signaling Technology, 1:200), IL13Rα2 (R&D system, 1:200), p-STAT3 (Cell Signaling Technology, 1:200), CD11b (Abcam, 1:400), CD33 (Zymed, 1:200) antibodies or isotype-matched IgG controls overnight at 4 °C. A positive slide was set at each experiment. Subsequently, a secondary biotinylated immunoglobulin G antibody solution and an avidin–biotin peroxidase reagent were added onto the slides. After washing with phosphate buffer saline, 3,3′-diaminobenzidine tetrachloride was added to the sections, followed by counterstaining with Mayer's hematoxylin. The immunohistochemical staining was scanned using an Aperio ScanScope CS whole slice scanner (Vista, CA, USA) with background subtraction as previously described [21]. The membrane, nuclear, or pixel immunohistochemical staining was quantified using Aperio Quantification software. The histoscore of the membrane and nuclear staining quantification were assessed according to the formula $(3 + \text{percent cells}) \times 3 + (2 + \text{percent cells}) \times 2 + (1 + \text{percent cells}) \times 1$, and the formula total intensity/total cell number was used to assess the histoscore of pixel quantification. In this case, the normalized score is between 0 and 300. This method has previously been described [22]. The immunohistochemical staining histoscores were converted to the range of −3 to 3 using Microsoft Excel software as previously described [23]. Cluster 3.0 with average linkage based on Pearson's correlation coefficient was used for hierarchical analysis, and the results were visualized using Java TreeView1.0.5.

Statistical analysis

All values are expressed as the means ± SEM. The statistical data analysis was performed using GraphPad Prism 5.03 (GraphPad Software, Inc., La Jolla, CA) statistical package. The differences in immunostaining and protein levels among each group were analyzed by the one-way ANOVA followed by the post-Tukey or Bonferroni multiple comparison tests. Student's t test was used for two-group analysis. The survival curves were plotted using Kaplan–Meier and log-rank tests. The Cox proportional hazard model was used for multivariate analysis to assess the significance of overall survival differences. Statistical significance was defined as a p value <0.05.

Results

## Overexpression of VISTA in OSCC compared with normal mucosa and epithelial dysplasia

To determine whether VISTA expression was associated with OSCC in humans, we searched the publicly available cancer dataset using the Oncomine database [24]. In Peng's head and neck cancers gene expression profiling dataset [25], the *C10orf54* (encoding VISTA) DNA copy number was significantly increased in OSCC compared with the controls ($p < 0.05$, Supplementary Fig. 1). To characterize the expression of VISTA in normal mucosa, epithelial dysplasia and OSCC, we quantified the immunohistochemical staining of the whole slide using Aperio ScanScope as previously described [26, 27]. Immunohistochemical analysis revealed that VISTA was highly expressed in primary OSCC ($n = 165$). VISTA was highly expressed on tumor-infiltrating immune cells in OSCC. The expressions of VISTA were markedly weak or negative in epithelial dysplasia ($n = 48$, $p < 0.01$) and normal mucosa ($n = 43$, $p < 0.01$, Fig. 1a, b).

Clinical significance of VISTA expression in human OSCC

To evaluate the clinical and pathological significance of VISTA expression in human OSCC, one-way ANOVA and Student's t test were used, and survival curves were plotted using the method of Kaplan–Meier and log-rank test. The results showed that VISTA expression was significantly correlated with lymph node status (N0 vs. N1 + N2; $p < 0.05$, Fig. 1c) but not tumor size (T1 + T2 vs. T3 + T4; $p > 0.05$, Fig. 1d) or pathological grade (I, II and III; $p > 0.05$, Fig. 1e). Furthermore, the difference of VISTA expression between metastatic lymph nodes and primary OSCC was not significant (OSCC vs. LN; $p > 0.05$, Supplementary Fig. 2a). There were no significant differences between primary OSCC and recurrent OSCC (OSCC vs. recurrence; $p > 0.05$, Supplementary Fig. 2b), pre-surgical radiotherapy (OSCC vs. RT; $p > 0.05$, Supplementary Fig. 2c), and pre-surgical inductive chemotherapy (OSCC vs. TPF; $p > 0.05$, Supplementary Fig. 2d). Moreover, no significant differences were observed between VISTA expression and human papillomavirus (HPV) infection status (HPV+ vs. HPV−; $p > 0.05$, Supplementary Fig. 2e), smoking habit (smoking vs. non-smoking; $p > 0.05$, Supplementary Fig. 2f), or drinking habit (drinking vs. non-drinking; $p > 0.05$, Supplementary Fig. 2g) in primary OSCC.

Further investigation of the role of VISTA expression in prognostic prediction revealed different VISTA/CD8 expression patterns in primary OSCC. As shown

Fig. 1 Increased expression of VISTA in human OSCC. **a** Representative hematoxylin and eosin (H&E) and immunohistochemical staining of VISTA in OSCC tissue compared with normal mucosa. *Scale bar* 50 μm. **b** Quantification of the immunohistochemical histoscore of VISTA among oral mucosa ($n=43$), dysplasia (Dys, $n=48$) and oral squamous cell carcinoma (OSCC, $n=165$). **c** Quantification of the immunohistochemical histoscore of VISTA between N0 and N1 + N2. **d** Quantification of the immunohistochemical histoscore of VISTA between T1 + T2 and T3 + T4 ($p>0.05$). **e** Quantification of the immunohistochemical histoscore of VISTA in pathological grade (I, II and III; $p>0.05$). All data are presented as the means ± SEM. *$p<0.05$; **$p<0.01$
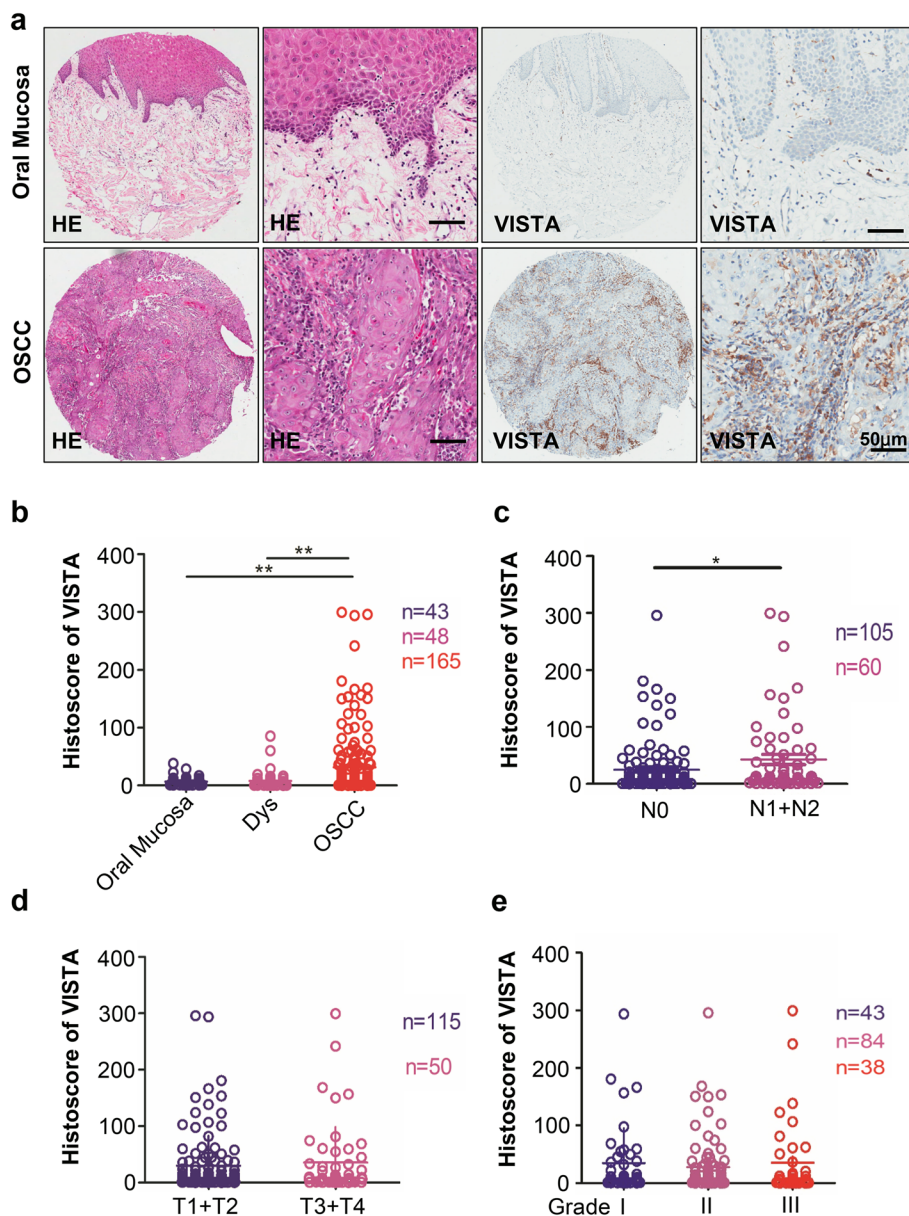
in Fig. 2, there were four types of VISTA/CD8 expression, namely, VISTA^{low}CD8^{low} (VL CL, Patient #1, Fig. 2a), VISTA^{high}CD8^{high} (VH CH, Patient #2, Fig. 2b), VISTA^{low}CD8^{high} (VL CH, Patient #3, Fig. 2c), and VISTA^{high}CD8^{low} (VH CL, Patient #4, Fig. 2d). The difference in overall survival was assessed using the Kaplan–Meier curve and log-rank test. In 165 primary OSCCs with follow-up data, no significant difference in the overall survival rate was observed between the VISTA high and VISTA low groups ($p=0.8799$, Fig. 3a). However, CD8 low expression could predict poor prognosis in primary OSCC ($p=0.0498$, Fig. 3b). The median of VISTA expression (histoscore = 7.54) and CD8 expression (histoscore = 23.87) were selected as cut-off values. Interestingly, the VH CL group ($n=22$) significantly predicted

poor prognosis compared with the VL CH group ($n=21$, Fig. 3c), while there were no differences between the VL CL and VH CH groups (Fig. 3d) and between the VL CH, VH CH and VL CL groups (Fig. 3e). Remarkably, the VH CL group, representing 13.3% (22/165) of the primary OSCCs, had significantly poorer prognosis compared with the other groups combined ($p=0.0119$ VH CL vs. VL CL and VH CH, Fig. 3f, $p=0.0079$ VH CL vs. VL CH and VH CH and VL CL, Fig. 3g). Considering that VISTA expression was correlated with lymph node status, we performed multivariate analysis using a Cox proportional hazard regression model to further disclose whether the poor prognosis of the VH CL subgroup depended on tumor size, pathological grade, and lymph node status. The results for CD8 ($p=0.052$, hazard ratio = 0.579, 95%

Fig. 2 Immunohistochemical staining of human OSCC tissues using anti-VISTA and anti-CD8 antibodies. Representative staining patterns of VISTA low and CD8 low (patient #1, **a**), VISTA high and CD8 high (patient #2, **b**), VISTA low and CD8 high (patient #3, **c**) and VISTA high and CD8 low (patient #4, **d**) are shown. *Scale bar* 50 μm
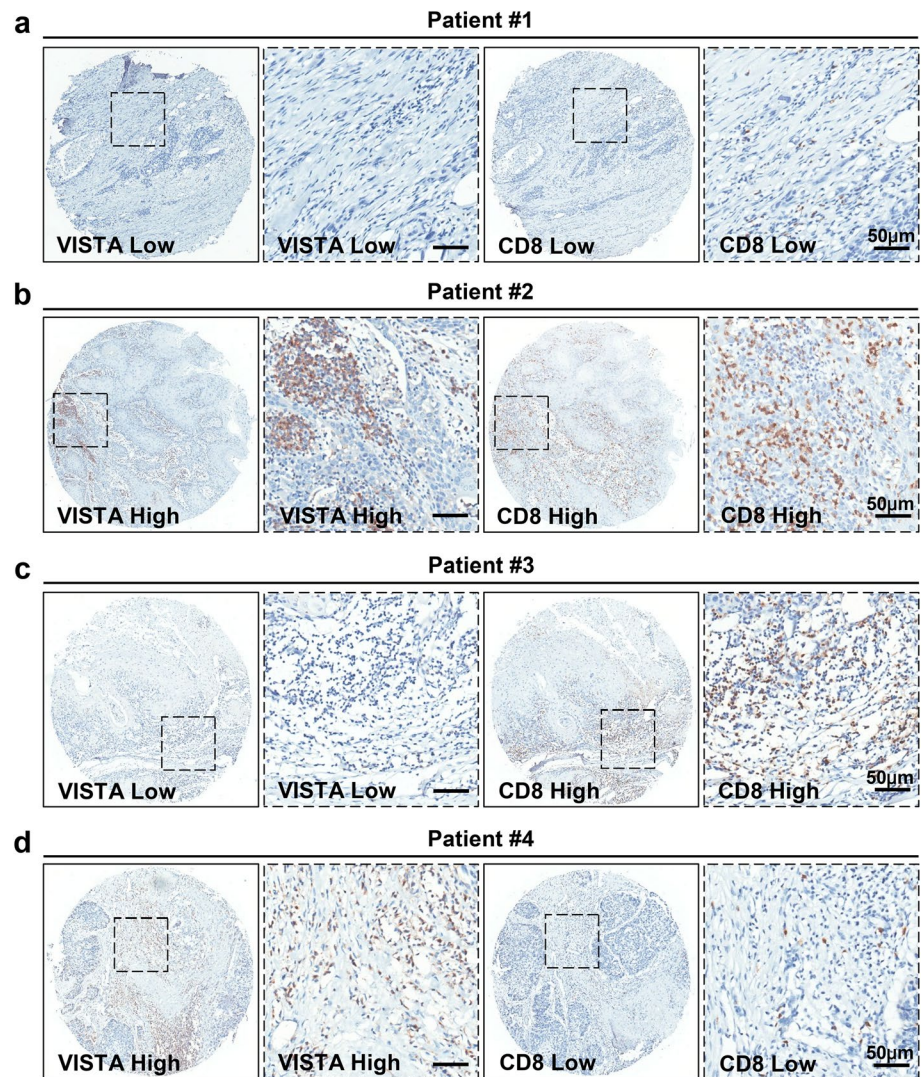

confidence interval = 0.333–1.005) in the multivariate analysis are shown in Supplementary Table 2. Moreover, the poor prognosis of the VH CL group was not dependent on larger tumor size, advanced pathological grade or positive lymph node status (Table 1) in primary OSCC in the present cohort.

Increased expression of VISTA correlated with PD-L1, CTLA-4, IL13Rα2, PI3K, p-STAT3 and MDSC markers in OSCC

A recent report showed VISTA overexpression in myeloid cells, such as CD11b^{+} cells, and combined treatment with VISTA and PD-L1 or CTLA-4 may synergistically augment antitumor effects [8, 14]. In the preliminary investigation of the molecules potentially associated with VISTA in the tumor microenvironment, we observed that VISTA expression was associated with MDSC markers (CD11b and CD33), PD-L1 and CTLA-4 using tissue

microarray screening. Additionally, VISTA was associated with Phospho-STAT3 at Tyrosine 705 (p-STAT3), PI3Kα p110 and IL13Rα2. Immunohistochemical staining showed that CTLA-4, CD11b and CD33 were highly expressed on the tumor-infiltrating immune cells in the tumor microenvironment (Fig. 4a). p-STAT3 was expressed in the nuclei of both tumor cells and immune cells (Fig. 4a). The expressions of PD-L1, PI3K, and IL13Rα2 were observed in OSCC cells (Fig. 4a). Hierarchical clustering revealed that VISTA expression was closely associated with that of IL13Rα2, CD11b and CD33 (Fig. 4b). Interestingly, Pearson's correlation coefficient test revealed that VISTA expression was statistically associated with PD-L1 ($p < 0.0001$, $r = 0.3432$), CTLA-4 ($p < 0.0001$, $r = 0.2535$), IL13Rα2 ($p < 0.0001$, $r = 0.2941$), PI3K ($p = 0.0016$, $r = 0.1963$), p-STAT3 ($p = 0.0024$, $r = 0.1889$), CD11b ($p < 0.0001$, $r = 0.2794$) and CD33 ($p = 0.0014$, $r = 0.1990$) (Fig. 5).

Fig. 3 Overall survival analysis of patients with OSCC according to the expression of VISTA and CD8. **a** Kaplan–Meier curves according to low and high expression of VISTA (VL and VH). **b** Kaplan–Meier curves according to low and high expression of CD8 (CL and CH). **c**–**f** Kaplan–Meier curves according to the combination of expressions of VISTA and CD8; VL CH vs. VH CL (**c**), VL CL vs. VH CH (**d**), VL CH vs. VH CH and VL CL (**e**), VH CL vs. VL CL and VH CH (**f**). **g** Kaplan–Meier curves according to the combination of expressions of VH CL vs. VL CH and VH CH and VL CL. *p < 0.05; **p < 0.01
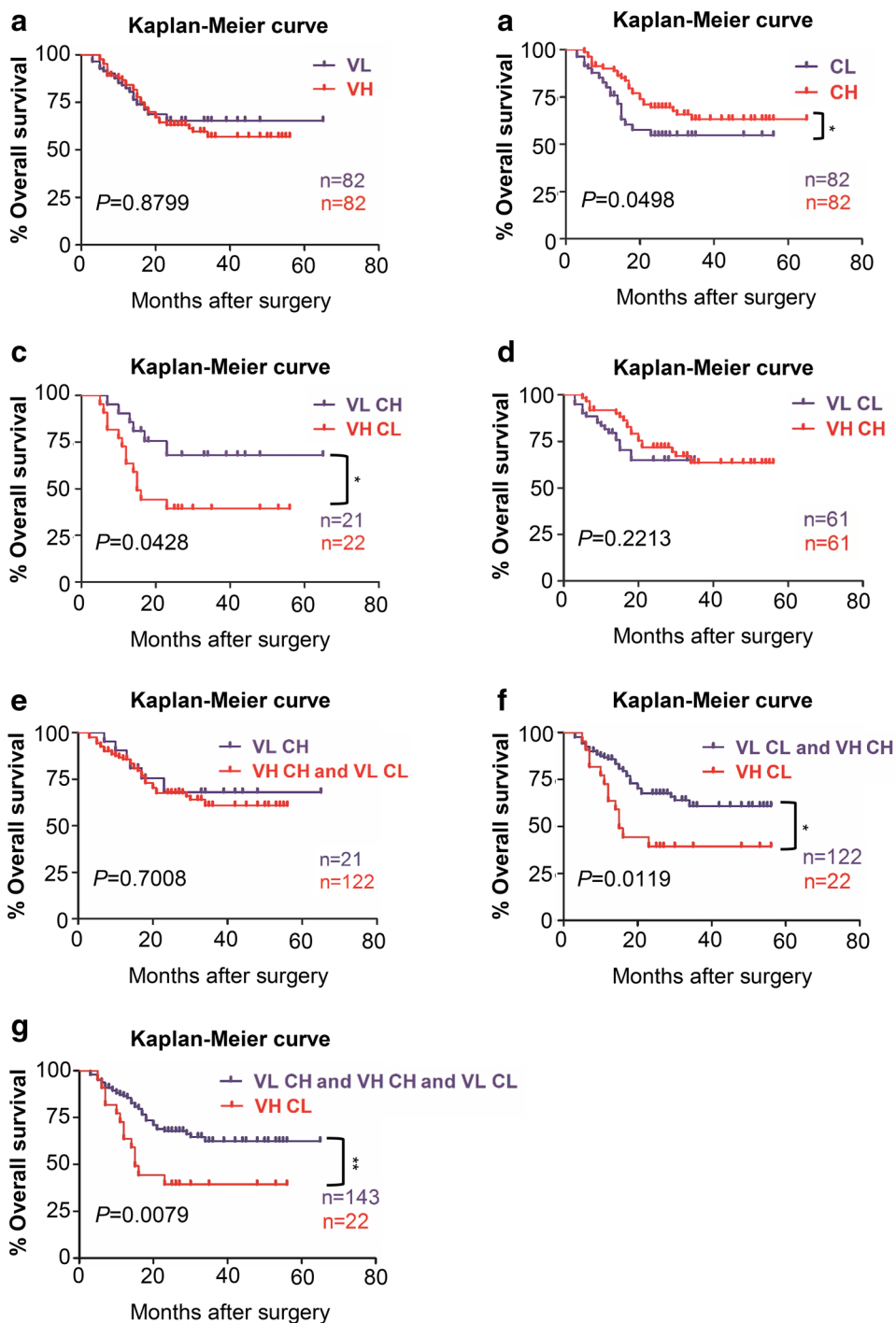
Discussion

VISTA is a novel immune checkpoint molecule, and the relevance of this molecule in tumors has rarely been reported. In the present study, we first demonstrated that VISTA protein expression was significantly higher in human OSCC specimens than in normal oral mucosa or dysplasia. Interestingly, VISTA expression in primary OSCC was correlated with lymph node status. Remarkably, a small subgroup of OSCC patients with VISTA high and CD8 low expression had significantly poorer overall survival compared with the other subgroups in the primary OSCC patients in the present cohort. Additionally, VISTA protein expression was correlated with MDSC markers (CD11b and CD33). VISTA expression was significantly correlated with other immune checkpoint markers (PD-L1 and CTLA-4) and immune-related pathways (IL13Rα2, PI3K and p-STAT3) in OSCC.

Table 1 Multivariate analysis for overall survival in primary OSCC patients

Parameters	HR (95% CI)	p value
Tumor size		
T3 + T4 vs. T1 + T2	1.597 (0.912–2.797)	0.102
Grade		
I	1.000	1.000
II vs. I	7.700 (1.846–32.129)	0.005*
III vs. I	8.437 (1.926–36.951)	0.005*
Node stage		
N1 + N2 vs. N0	2.011 (1.164–3.475)	0.012*
VISTA CD8 expression		
VH CL vs. VH CH and VL CL and VL CH	1.971 (1.047–3.714)	0.036*

Cox proportional hazards regression model

HR hazard ratio, *95% CI* 95% confidence interval, *VH* VISTA high, *VL* VISTA low, *CH* CD8 high, *CL* CD8 low

*$p < 0.05$

It has been reported that tumor-infiltrating CD8$^+$ T cells are associated with prolonged survival in various tumor types such as colorectal cancer [28], endometrial adenocarcinoma [29], ovarian cancer [30], renal cell cancer [31] and esophageal cancer [32]. Consistent with these studies, the data in the present study indicated that tumor-infiltrating CD8$^+$ T cells might be associated with a good prognosis in OSCC. The prognostic value of VISTA in cancers has not yet been elucidated. The results of the present study demonstrated that VISTA was not a significant prognostic indicator for OSCC. Interestingly, the survival analysis of VISTA in combination with CD8 expression in the primary OSCC demonstrated that patients with VISTA high and CD8 low had a poorer prognosis than other patients in the present cohort, indicating that VISTA high and CD8 low may represent an immunosuppressive status in the tumor microenvironment. Notably, the Cox multivariate analysis also showed that VISTA, in cooperation with CD8, was an independent factor to predict the survival of OSCC, independent of tumor size, lymph node status, and pathological grade in the primary OSCC of the present cohort. Although the VISTA high CD8 low subgroup had poor prognosis in

Fig. 4 High expression of CD11b, CD33, CTLA-4, p-STAT3, PI3K, IL13Rα2, PD-L1 and VISTA in OSCC. **a** Representative immunohistochemical staining of CD11b, CD33, CTLA-4, p-STAT3, PI3K, IL13Rα2, PD-L1 and VISTA in OSCC tissue. *Scale bar* 50 μm. **b** Hierarchical clustering of CD11b, CD33, CTLA-4, PI3Kα p110, IL13Rα2, p-STAT3, PD-L1 and VISTA immunohistochemical results in human OSCC with statistics including mucosa, dysplasia and primary OSCC (total $n = 256$)
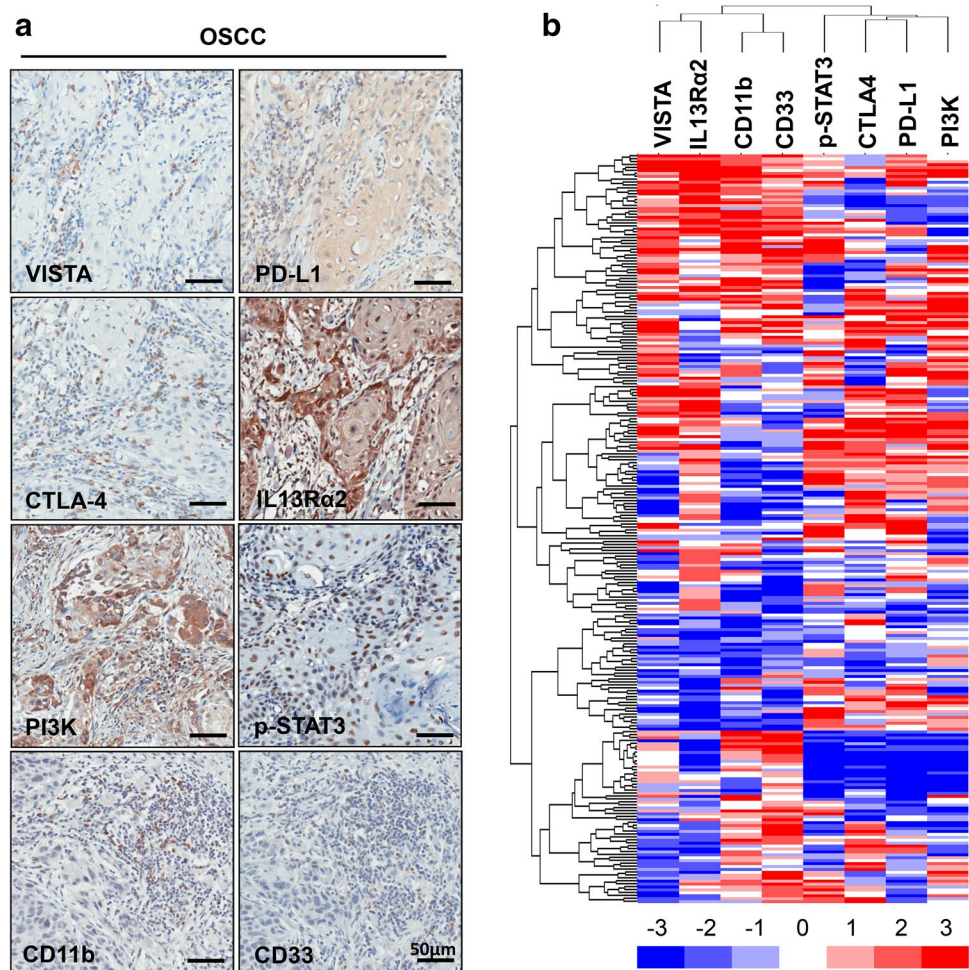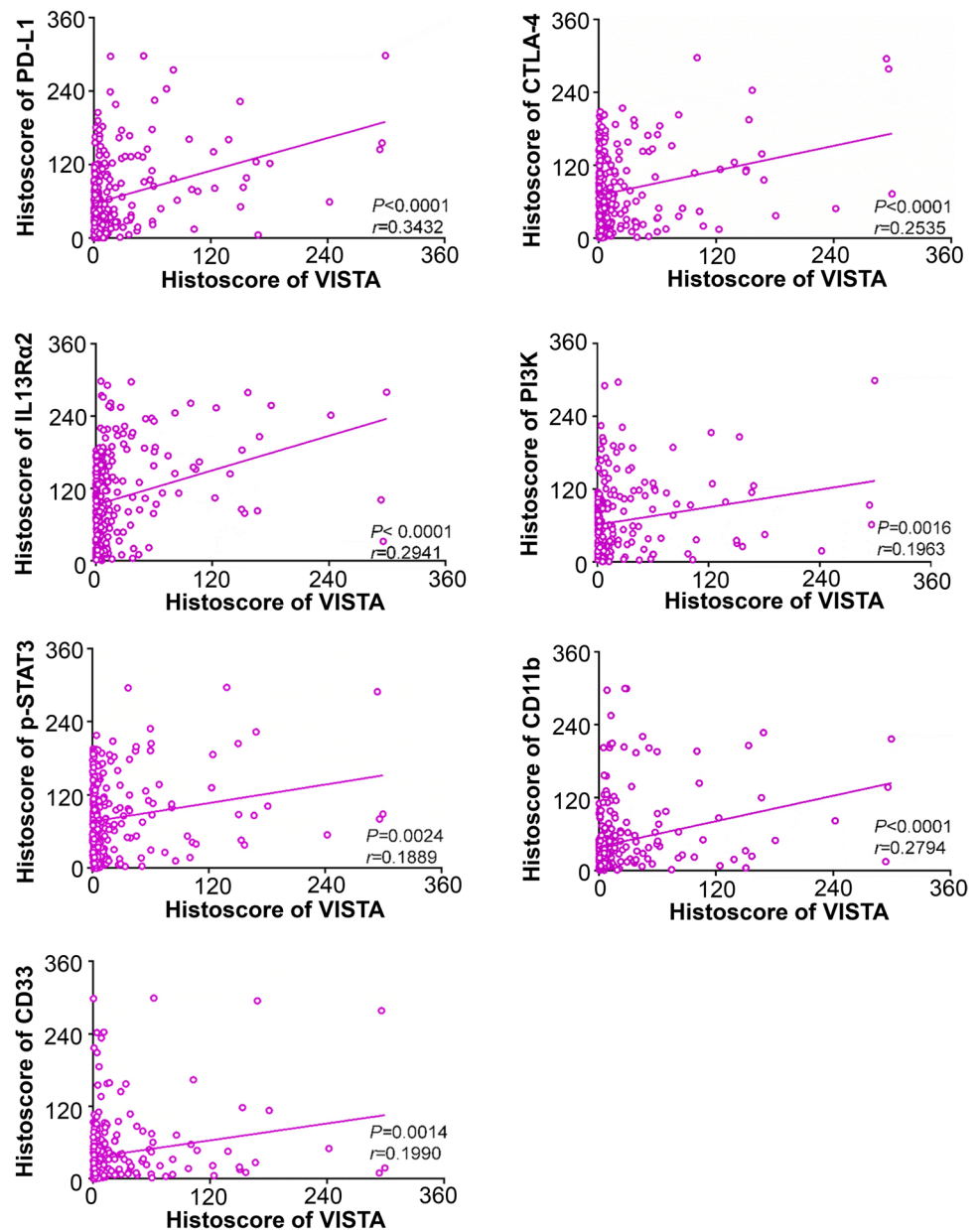
the present study, it should be cautiously assumed based on the small population that VISTA synergized with CD8 may be a novel clinical prognostic parameter for OSCC.

Immune checkpoints and suppressive immune cells, such as MDSCs, regulatory T cells (Tregs) and tumor-associated macrophages (TAMs), play crucial roles in suppressing tumor-specific T cell responses, enabling cancer cells to evade immune surveillance in the OSCC microenvironment [33, 34]. Recent evidence has shown that VISTA, different from PD-1 and CTLA-4, is primarily expressed on CD11b myeloid cells such as myeloid dendritic cells and MDSCs, indicating that VISTA plays a role in tumor evasion from the immune system [14, 15, 35]. The present study showed that VISTA was highly expressed on tumor-infiltrating

immune cells in OSCC, and the results also demonstrated that the expression of VISTA was statistically associated with MDSC markers (CD11b and CD33), suggesting that VISTA may play a role in the immune system of OSCC.

Thus far, little is known about the molecular regulation of VISTA. Thus, we preliminarily explored the molecules potentially associated with VISTA in the tumor microenvironment. In the present study, using tissue microarray screening, we observed that VISTA protein expression was correlated with IL13Rα2, PI3K and p-STAT3, which were highly expressed or activated in human OSCC [19, 36]. Additionally, IL13Rα2 overexpression in human cancer was associated with increased TGF-β1 [37], an important cytokine in the tumor metastasis and recruitment of

MDSCs [33]. A recent report indicated the activation of p-STAT3 prevented the maturation of myeloid cells [38], and other studies have reported that PD-L1 expression was driven through the STAT3 or PI3K-AKT signaling pathway [39]. A previous study revealed that the VISTA-synergized PD-L1 checkpoint blockade generated optimal antitumor immunity in cancer [40]. Other studies have also reported that blockade could attenuate tumor growth, particularly when combined with a cancer vaccine [14]. Interestingly, PD-L1 and CTLA-4 were particularly overexpressed in OSCC [27, 41] and VISTA was positively correlated with PD-L1 and CTLA-4. Based on these findings, we hypothesized that VISTA was likely to have immune functions and may be a novel target in combination with other immune checkpoints for cancer immunotherapy. Further studies are needed to explore the function and immunological mechanisms of VISTA once a commercial anti-VISTA monoclonal antibody is available.

In conclusion, the results of the present study showed that VISTA is overexpressed in OSCC and is correlated with PD-L1, CTLA-4, IL13Rα2, PI3K, p-STAT3 and MDSC markers (CD11b and CD33), indicating that VISTA, as an immune checkpoint molecule, may regulate antitumor immunity in OSCC. Furthermore, VISTA and CD8 may collaboratively predict the survival of OSCC. Thus, these observations demonstrated that VISTA might be a potential antitumor target for OSCC.

Compliance with ethical standards

Conflict of interest The authors declare that they have no conflict of interest.

References

1. Leemans CR, Braakhuis BJ, Brakenhoff RH (2011) The molecular biology of head and neck cancer. Nat Rev Cancer 11(1):9–22. doi:10.1038/nrc2982

2. Smith RB, Sniezek JC, Weed DT, Wax MK (2007) Utilization of free tissue transfer in head and neck surgery. Otolaryngol Head Neck Surg 137(2):182–191. doi:10.1016/j.otohns.2007.04.011

3. Vergeer MR, Doornaert PA, Rietveld DH, Leemans CR, Slotman BJ, Langendijk JA (2009) Intensity-modulated radiotherapy reduces radiation-induced morbidity and improves health-related quality of life: results of a nonrandomized prospective study using a standardized follow-up program. Int J Radiat Oncol Biol Phys 74(1):1–8. doi:10.1016/j.ijrobp.2008.07.059

4. Boscolo-Rizzo P, Maronato F, Marchiori C, Gava A, Da Mosto MC (2008) Long-term quality of life after total laryngectomy and postoperative radiotherapy versus concurrent chemoradiotherapy for laryngeal preservation. Laryngoscope 118(2):300–306. doi:10.1097/MLG.0b013e31815a9ed3

5. Hashemi-Sadraei N, Sikora AG, Brizel DM (2016) Immunotherapy and checkpoint inhibitors in recurrent and metastatic head and neck cancer. Am Soc Clin Oncol Educ Book 35:e277–e282. doi:10.14694/EDBK_157801

6. Lesterhuis WJ, Haanen JB, Punt CJ (2011) Cancer immunotherapy—revisited. Nat Rev Drug Discov 10(8):591–600. doi:10.1038/nrd3500

7. Kloke BP, Mahr A, Jabulowsky RA, Kutscher S, Rae R, Britten CM (2015) Cancer immunotherapy achieves breakthrough status: 12th annual meeting of the association for cancer immunotherapy (CIMT), Mainz, Germany, May 6–8, 2014. Cancer Immunol Immunother 64(7):923–930. doi:10.1007/s00262-014-1643-7

8. Topalian SL, Drake CG, Pardoll DM (2015) Immune checkpoint blockade: a common denominator approach to cancer therapy. Cancer Cell 27(4):450–461. doi:10.1016/j.ccell.2015.03.001

9. Greenwald RJ, Freeman GJ, Sharpe AH (2005) The B7 family revisited. Annu Rev Immunol 23:515–548. doi:10.1146/annurev.immunol.23.021704.115611

10. Blank C, Gajewski TF, Mackensen A (2005) Interaction of PD-L1 on tumor cells with PD-1 on tumor-specific T cells as a mechanism of immune evasion: implications for tumor immunotherapy. Cancer Immunol Immunother 54(4):307–314. doi:10.1007/s00262-004-0593-x

11. Simeone E, Ascierto PA (2012) Immunomodulating antibodies in the treatment of metastatic melanoma: the experience with anti-CTLA-4, anti-CD137, and anti-PD1. J Immunotoxicol 9(3):241–247. doi:10.3109/1547691X.2012.678021

12. Gunturi A, McDermott DF (2014) Potential of new therapies like anti-PD1 in kidney cancer. Curr Treat Options Oncol 15(1):137–146. doi:10.1007/s11864-013-0268-y

13. Westin JR, Chu F, Zhang M, Fayad LE, Kwak LW, Fowler N, Romaguera J, Hagemeister F, Fanale M, Samaniego F, Feng L, Baladandayuthapani V, Wang Z, Ma W, Gao Y, Wallace M, Vence LM, Radvanyi L, Muzzafar T, Rotem-Yehudar R, Davis RE, Neelapu SS (2014) Safety and activity of PD1 blockade by pidilizumab in combination with rituximab in patients with relapsed follicular lymphoma: a single group, open-label, phase 2 trial. Lancet Oncol 15(1):69–77. doi:10.1016/S1470-2045(13)70551-5

14. Wang L, Rubinstein R, Lines JL, Wasiuk A, Ahonen C, Guo Y, Lu LF, Gondek D, Wang Y, Fava RA, Fiser A, Almo S, Noelle RJ (2011) VISTA, a novel mouse Ig superfamily ligand that negatively regulates T cell responses. J Exp Med 208(3):577–592. doi:10.1084/jem.20100619

15. Flies DB, Wang S, Xu H, Chen L (2011) Cutting edge: a monoclonal antibody specific for the programmed death-1 homolog prevents graft-versus-host disease in mouse models. J Immunol 187(4):1537–1541. doi:10.4049/jimmunol.1100660

16. Le Mercier I, Chen W, Lines JL, Day M, Li J, Sergent P, Noelle RJ, Wang L (2014) VISTA regulates the development of protective antitumor immunity. Cancer Res 74(7):1933–1944. doi:10.1158/0008-5472.CAN-13-1506

17. Wang L, Le Mercier I, Putra J, Chen W, Liu J, Schenk AD, Nowak EC, Suriawinata AA, Li J, Noelle RJ (2014) Disruption of the immune-checkpoint VISTA gene imparts a proinflammatory phenotype with predisposition to the development of autoimmunity. Proc Natl Acad Sci USA 111(41):14846–14851. doi:10.1073/pnas.1407447111

18. Zhong LP, Zhang CP, Ren GX, Guo W, William WN Jr, Sun J, Zhu HG, Tu WY, Li J, Cai YL, Wang LZ, Fan XD, Wang ZH, Hu YJ, Ji T, Yang WJ, Ye WM, Li J, He Y, Wang YA, Xu LQ, Wang BS, Kies MS, Lee JJ, Myers JN, Zhang ZY (2013) Randomized phase III trial of induction chemotherapy with docetaxel, cisplatin, and fluorouracil followed by surgery versus up-front surgery

in locally advanced resectable oral squamous cell carcinoma. J Clin Oncol 31(6):744–751. doi:10.1200/JCO.2012.43.8820

19. Bu LL, Zhao ZL, Liu JF, Ma SR, Huang CF, Liu B, Zhang WF, Sun ZJ (2015) STAT3 blockade enhances the efficacy of conventional chemotherapeutic agents by eradicating head neck stemloid cancer cell. Oncotarget 6(39):41944–41958. doi:10.18632/oncotarget.5986

20. Lyford-Pike S, Peng S, Young GD, Taube JM, Westra WH, Akpeng B, Bruno TC, Richmon JD, Wang H, Bishop JA, Chen L, Drake CG, Topalian SL, Pardoll DM, Pai SI (2013) Evidence for a role of the PD-1:PD-L1 pathway in immune resistance of HPV-associated head and neck squamous cell carcinoma. Cancer Res 73(6):1733–1741. doi:10.1158/0008-5472.CAN-12-2384

21. Czerninski R, Amornphimoltham P, Patel V, Molinolo AA, Gutkind JS (2009) Targeting mammalian target of rapamycin by rapamycin prevents tumor progression in an oral-specific chemical carcinogenesis model. Cancer Prev Res (Phila) 2(1):27–36. doi:10.1158/1940-6207.CAPR-08-0147

22. Sun ZJ, Zhang L, Hall B, Bian Y, Gutkind JS, Kulkarni AB (2012) Chemopreventive and chemotherapeutic actions of mTOR inhibitor in genetically defined head and neck squamous cell carcinoma mouse model. Clin Cancer Res 18(19):5304–5313. doi:10.1158/1078-0432.CCR-12-1371

23. Ma SR, Wang WM, Huang CF, Zhang WF, Sun ZJ (2015) Anterior gradient protein 2 expression in high grade head and neck squamous cell carcinoma correlated with cancer stem cell and epithelial mesenchymal transition. Oncotarget 6(11):8807–8821. doi:10.18632/oncotarget.3556

24. Rhodes DR, Kalyana-Sundaram S, Mahavisno V, Varambally R, Yu J, Briggs BB, Barrette TR, Anstet MJ, Kincead-Beal C, Kulkarni P, Varambally S, Ghosh D, Chinnaiyan AM (2007) Oncomine 3.0: genes, pathways, and networks in a collection of 18,000 cancer gene expression profiles. Neoplasia 9(2):166–180

25. Peng CH, Liao CT, Peng SC, Chen YJ, Cheng AJ, Juang JL, Tsai CY, Chen TC, Chuang YJ, Tang CY, Hsieh WP, Yen TC (2011) A novel molecular signature identified by systems genetics approach predicts prognosis in oral squamous cell carcinoma. PLoS One 6(8):e23452. doi:10.1371/journal.pone.0023452

26. Chen HH, Huang N, Chen YM, Chen TJ, Chou P, Lee YL, Chou YJ, Lan JL, Lai KL, Lin CH, Chen DY (2013) Association between a history of periodontitis and the risk of rheumatoid arthritis: a nationwide, population-based, case-control study. Ann Rheum Dis 72(7):1206–1211. doi:10.1136/annrheumdis-2012-201593

27. Yu GT, Bu LL, Huang CF, Zhang WF, Chen WJ, Gutkind JS, Kulkarni AB, Sun ZJ (2015) PD-1 blockade attenuates immunosuppressive myeloid cells due to inhibition of CD47/SIRPalpha axis in HPV negative head and neck squamous cell carcinoma. Oncotarget 6(39):42067–42080. doi:10.18632/oncotarget.5955

28. Pages F, Berger A, Camus M, Sanchez-Cabo F, Costes A, Molidor R, Mlecnik B, Kirilovsky A, Nilsson M, Damotte D, Meatchi T, Bruneval P, Cugnenc PH, Trajanoski Z, Fridman WH, Galon J (2005) Effector memory T cells, early metastasis, and survival in colorectal cancer. N Engl J Med 353(25):2654–2666. doi:10.1056/NEJMoa051424

29. Workel HH, Komdeur FL, Wouters MC, Plat A, Klip HG, Eggink FA, Wisman GB, Arts HJ, Oonk MH, Mourits MJ, Yigit R, Versluis M, Duiker EW, Hollema H, de Bruyn M, Nijman HW (2016) CD103 defines intraepithelial CD8+ PD1+ tumour-infiltrating lymphocytes of prognostic significance in endometrial adenocarcinoma. Eur J Cancer 60:1–11. doi:10.1016/j.ejca.2016.02.026

30. Hamanishi J, Mandai M, Iwasaki M, Okazaki T, Tanaka Y, Yamaguchi K, Higuchi T, Yagi H, Takakura K, Minato N, Honjo T, Fujii S (2007) Programmed cell death 1 ligand 1 and tumor-infiltrating CD8+ T lymphocytes are prognostic factors of human ovarian cancer. Proc Natl Acad Sci USA 104(9):3360–3365. doi:10.1073/pnas.0611533104

31. Nakano O, Sato M, Naito Y, Suzuki K, Orikasa S, Aizawa M, Suzuki Y, Shintaku I, Nagura H, Ohtani H (2001) Proliferative activity of intratumoral CD8(+) T-lymphocytes as a prognostic factor in human renal cell carcinoma: clinicopathologic demonstration of antitumor immunity. Cancer Res 61(13):5132–5136

32. Schumacher K, Haensch W, Roefzaad C, Schlag PM (2001) Prognostic significance of activated CD8(+) T cell infiltrations within esophageal carcinomas. Cancer Res 61(10):3932–3936

33. Ferris RL (2015) Immunology and Immunotherapy of Head and Neck Cancer. J Clin Oncol 33(29):3293–3304. doi:10.1200/JCO.2015.61.1509

34. De Costa AM, Schuyler CA, Walker DD, Young MR (2012) Characterization of the evolution of immune phenotype during the development and progression of squamous cell carcinoma of the head and neck. Cancer Immunol Immunother 61(6):927–939. doi:10.1007/s00262-011-1154-8

35. Lines JL, Pantazi E, Mak J, Sempere LF, Wang L, O'Connell S, Ceeraz S, Suriawinata AA, Yan S, Ernstoff MS, Noelle R (2014) VISTA is an immune checkpoint molecule for human T cells. Cancer Res 74(7):1924–1932. doi:10.1158/0008-5472.CAN-13-1504

36. Hall B, Nakashima H, Sun ZJ, Sato Y, Bian Y, Husain SR, Puri RK, Kulkarni AB (2013) Targeting of interleukin-13 receptor alpha2 for treatment of head and neck squamous cell carcinoma induced by conditional deletion of TGF-beta and PTEN signaling. J Transl Med 11:45. doi:10.1186/1479-5876-11-45

37. Fichtner-Feigl S, Strober W, Kawakami K, Puri RK, Kitani A (2006) IL-13 signaling through the IL-13alpha2 receptor is involved in induction of TGF-beta1 production and fibrosis. Nat Med 12(1):99–106. doi:10.1038/nm1332

38. Bu LL, Yu GT, Deng WW, Mao L, Liu JF, Ma SR, Fan TF, Hall B, Kulkarni AB, Zhang WF, Sun ZJ (2016) Targeting STAT3 signaling reduces immunosuppressive myeloid cells in head and neck squamous cell carcinoma. OncoImmunology 5(5):e1130206. doi:10.1080/2162402X.2015.1130206

39. Pardoll DM (2012) The blockade of immune checkpoints in cancer immunotherapy. Nat Rev Cancer 12(4):252–264. doi:10.1038/nrc3239

40. Liu J, Yuan Y, Chen W, Putra J, Suriawinata AA, Schenk AD, Miller HE, Guleria I, Barth RJ, Huang YH, Wang L (2015) Immune-checkpoint proteins VISTA and PD-1 nonredundantly regulate murine T-cell responses. Proc Natl Acad Sci USA 112(21):6682–6687. doi:10.1073/pnas.1420370112

41. Yu GT, Bu LL, Zhao YY, Mao L, Deng WW, Wu TF, Zhang WF, Sun ZJ (2016) CTLA4 blockade reduces immature myeloid cells in head and neck squamous cell carcinoma. OncoImmunology 5(6):e1151594. doi:10.1080/2162402X.2016.1151594